Original paper

Individualized 3D printing for skin cancer brachytherapy: Development, implementation, clinical applications, and treatment assessment

Michal Poltorak, MSc[1], Pawel Banatkiewicz, MD[1], Prof. Lukasz Poltorak, PhD[2], Piotr Sobolewski, MD, PhD[1,3], Damian Zimon, MD[1,3], Prof. Maciej Szwast, PhD[4], Prof. Irena Walecka, MD, PhD[1,3]

[1]The National Institute of Medicine of the Ministry of the Interior and Administration, Warsaw, Poland, [2]Electrochemistry@Soft Interfaces Team, Department of Inorganic and Analytical Chemistry, Faculty of Chemistry, University of Lodz, Lodz, Poland, [3]Department of Dermatology, Centre of Postgraduate Medical Education, Warsaw, Poland, [4]Department of Chemical and Process Engineering, Warsaw University of Technology, Warsaw, Poland

Abstract

Purpose: This study outlined the prevalent use of brachytherapy in skin cancers, such as basal cell carcinoma (BCC) and squamous cell carcinoma (SCC). The importance of customized applicator fabrication for optimal treatment delivery was highlighted, focusing on adaptable devices tailored to individual patient anatomy, often facilitated by 3D printing technology. The purpose of this work was to investigate the association of medical science and 3D printing in customized applicator fabrication for brachytherapy, leveraging the advancements in fabrication techniques to enhance treatment precision and patient outcomes.

Material and methods: The study enrolled five patients with tumor lesions unsuitable for surgical intervention, situated across various anatomical locations, such as earlobe, temple, hand, and cheek. Customized applicators were fabricated *via* 3D printing (fused deposition modeling) for each patient, followed by radiotherapy protocol delivering a total dose of 51 Gy in 17 fractions. Patient assessments during and post-radiotherapy were done by radiation oncologist using RTOG scale as well as dermatological evaluations with dermatoscopy and reflectance confocal microscopy. Methodologically, applicators were 3D-printed using fused deposition modeling technology. Printing parameters were optimized in Prusa Slicer software, ensuring precise control in printout shape correlated with treatment efficacy.

Results: This study examined the therapeutic outcomes of brachytherapy in five patients with inoperable skin cancer lesions. Utilizing customized 3D-printed applicators, the patients underwent brachytherapy regimen delivering a cumulative dose of 51 Gy in 17 fractions. The evaluation with RTOG scale revealed varied treatment responses, with complete remission achieved in all cases. Reflectance confocal microscopy showed post-treatment normalization of epidermal morphology and notable scar formation. Optical profilometry demonstrated consistent micro-structures on the applicator surfaces, without compromising treatment efficacy. These findings indicated the potential of 3D-printed applicators in optimizing brachytherapy outcomes in skin cancer management.

Conclusions: Our study demonstrates the effectiveness of 3D-printed applicators in treating inoperable skin cancer lesions with high precision. In personalized fabrication, optimal conformity with anatomical features was achieved, resulting in complete remission in all patients. This approach minimizes treatment-related side effects and enhances overall patient outcomes, suggesting a promising future for 3D printing technology in skin cancer treatment applications. Further research and clinical validation are needed to establish 3D printing as a standard practice in skin cancer treatment.

J Contemp Brachytherapy 2024; 16, 3: 173–183
DOI: https://doi.org/10.5114/jcb.2024.141420

Key words: superficial brachytherapy, 3D printing, fused deposition modeling, skin cancer, individual applicator.

Purpose

Brachytherapy is often selected in skin cancer cases where surgical intervention can result in significant cosmetic impacts on patients who require cosmetic or reconstructive procedures [1]. Among various treatment modalities, surgery or radiotherapy are routinely employed for this type of cancer [2-4]. Brachytherapy, a treatment option for skin cancer, involves placing a radiation source directly within or near the tumor while minimizing radia-

Address for correspondence: Michal Poltorak, MSc, The National Institute of Medicine of the Ministry of the Interior and Administration, Woloska 137, 02-507 Warsaw, Poland,
e-mail: michal.poltorak@cskmswia.gov.pl

Received: 10.04.2024
Accepted: 26.06.2024
Published: 30.06.2024

tion exposure to surrounding healthy tissues [5-10]. Skin cancer, especially basal cell carcinoma (BCC) and squamous cell carcinoma (SCC), are among the most common types of cancer worldwide, with reported annual increases in their prevalence [11-14]. When brachytherapy is employed as the treatment method, the choice of applicator significantly impacts the treatment process. Therefore, the primary intent is to utilize adaptable devices capable of being customized to fit the unique topography of each patient skin, ensuring optimal treatment delivery (e.g., lack of air gaps). One of the tools that can be used to achieve this is computed tomography-based (CT) skin surface imaging, combined with 3D printing technology. With additive manufacturing, customized applicators can be created to match specific contours and dimensions of individual patient skin. Brachytherapy offers precise tumor control, and can improve cosmetic outcomes while maintaining treatment standards [15]. This targeted approach minimizes damage to healthy tissues, making it a valuable option in modern oncology. Optimizing various clinical parameters, such as total dose, fraction dose, target area size, and overall treatment duration is crucial before initiating skin cancer treatment with a radioactive source, as these factors greatly influence the ultimate treatment outcome [16].

3D printing technology is progressively gaining momentum in an increasing number of scientific domains. In recent years, advanced do-it-yourself (DIY) fabrication of scientific components has become feasible with very little effort. This tendency overlaps with the market accessibility of affordable (or even cheap) printers, which provide very good printing resolutions. Current scientific literature is full of interesting applications of ready-to-use functional and 3D-printed (frequently fully) objects [17]. There are review papers describing applications of 3D printing in chemistry [18, 19], bio-based research [20, 21], electronics [22], construction engineering [23], among many other examples. The combination of medical science and 3D-based technology opens new possibilities explored by scientists of different domains. In this respect, the most frequently used 3D printing technologies include fused deposition modeling [24], stereolithography [25], and bio-printing [26]. A few specific examples are described below. Eichholz *et al*. proved the beneficial effect of 3D-printed scaffolds during bone defect healing, as studied *in vivo* in rats and used as a model. In their work, melt electro-writing using polycaprolactone was combined with fused deposition modeling 3D printing based on polylactic acid, to create the core and the shell of the scaffold, respectively [27]. Another advancement is the customized production of implants created with post-processed computer tomography imaging, or simple implants for drug delivery platforms. These can be prepared using thermoplastics [28, 29] and metals (very demanding in processing), such as titanium [30, 31]. We also believe that in the near future, 3D printing will be routinely used in customized applicator fabrication for brachytherapy. Skin areas affected by cancer can be easily converted into 3D maps followed by CT imaging. It has been already proven that materials, such as polylactic acid (PLA) or acrylonitrile butadiene styrene (ABS) can be successfully employed in applicator printing [32, 33]. Ricotti *et al*. studied the effect of printout infill percentage on the dosimetry response, and observed that the low infill density is still suitable for brachytherapy applications; the measured dose distribution for 3D-printed and commercial applications are in good agreement [33].

In the current study, a coherent description of all stages of brachytherapy treatment was presented, including scanning of the skin affected by cancer, applicator shape optimization, 3D printing, radiation treatment, and obtained results assessment.

Material and methods

The study included five patients enrolled based on the presence of tumor lesions ineligible for surgical interventions. Lesions were situated on the earlobe of the right auricle, the left temple, the internal surface of the right hand, and the right cheek. Customized applicators were fabricated *via* 3D printing for each patient. Subsequently, patients underwent a radiotherapy protocol delivering a total dose of 51 Gy in 17 fractions (3 Gy each fraction). During and post-radiotherapy, patients were subjected to observation by a radiation oncologist and medical physicist using Radiation Therapy Oncology Group (RTOG) scale, along with dermatology specialists utilizing dermatoscopy, video-dermatoscopy, and reflectance confocal microscopy. Applicators were individualized for each patient, ensuring that no other patient could use the same applicator. New medical-grade foil was utilized during each fraction to prevent direct contact between the applicator material and patient skin in irradiation area. The applicator was kept during the therapy in a dedicated individual container, and if sterilization was required due to material contamination, ethylene oxide (ETO) sterilization was applied.

This study aimed to comprehensively evaluate treatment plan parameters for skin cancer treatment, particularly focusing on those relevant to 3D printing. Also, this research aimed to analyze the clinical parameters of treatment plans commonly used in clinical practice, including V_{100} (%), V_{150} (%), D_{90} (Gy), V_{PTV} (cm^3), and coverage index (CI) parameter, while gathering information on printing time, filament usage, and the number of catheters employed for 3D-printed applicators.

Applicators were 3D-printed using common fused deposition modeling-based technology. Prusa iMk3+ was used as the 3D printer. Hardware (the experimentally variable parts) was composed of the nozzle with a diameter of 0.4 mm, polyethyleneimine (PEI) smooth pad that served as the support for applicators, and the cover that prevented from possible wind blows. Before all printing operations, the pad was thoroughly rinsed with isopropyl alcohol to degrease the surface and remove polymeric debris. All applicators were printed with polylactic acid-based filaments (Fiberology® specifications: table pad temperature, 60°C; nozzle temperature, 210-215°C). Applicators .stl files were created by CT scans of the part of a patient body affected by cancerous changes data treatment. All applicators printing pro-

cedures were first optimized, and starting parameters were provided. These were then slightly changed for the specific applicator. All these were done in Prusa Slicer software, in which the following parameters varied: nozzle temperature (from 210°C to 215°C, with 215°C used during final applicator fabrication); type of the support applied for unsupported parts of the printout (grid); pattern of the support (rectilinear); pattern spacing varied from 1 to 6 mm (3 mm was applied); number of vertical and horizontal shells (3 for vertical shells perimeters, 9 on the top, and 7 on the bottom solid horizontal shells layers); 0.15 quality was chosen as the printing settings; and 100% infill was used to avoid any larger air gaps in the printed applicator. The orientation of the applicator vs. the support and location of the supporting material were utilized for every applicator manually in Prusa Slicer software. Once all the parameters were adjusted, g-code was generated and used for the applicator fabrication.

Geometrical parameters of capillaries were studied using 3D optical profilometer (UP-3000, Rtec Instruments, USA). 20× objective was used for visualization in the confocal mode, and MountainView software was employed for the obtained images post-treatment.

Treatment planning system (TPS) and applicator design

For each patient, customized applicators were meticulously fabricated *via* 3D printing to ensure precise conformity to individual anatomical features. Subsequently, they underwent a rigorously planned radiotherapy protocol, with a total dose of 51 Gy delivered in 17 fractions (3 Gy each fraction). Treatment planning was executed with BrachyVision version 16.1 (Varian Medical Systems, Palo Alto, CA, USA). Home-made software was employed to convert high-resolution CT scans with a drawn structure of the cancer-affected body part into .stl files representing the applicator design. Next, the advanced capabilities of Prusa Slicer software were employed to translate the .stl file into intricate g-code instructions. Manual adjustment of applicator supports was undertaken with precise attention to detail, aiming at minimizing potential surface defects while ensuring the flawless printability and structural integrity of the final product.

Figure 1 presents an exemplary dose distribution for patient No. 2 using personalized treatment plan with an individualized applicator. This tailored approach optimized therapeutic efficacy and minimized potential side

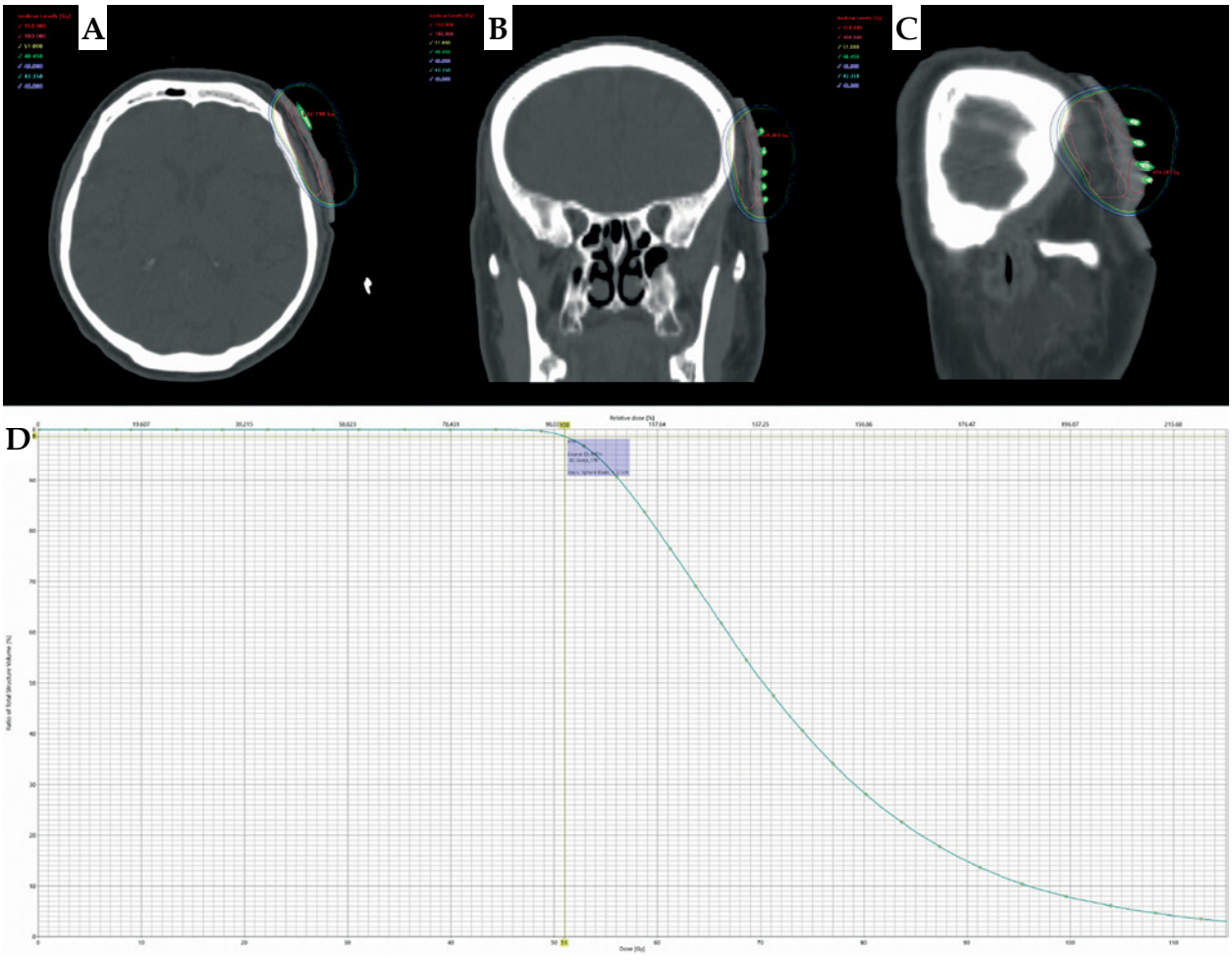

Fig. 1. Dose distribution with 3D-printed applicator for **A**) transverse section, **B**) frontal section, and **C**) sagittal section. **D**) Dose volume histogram (DVH) with target structure

effects, thereby enhancing patient outcomes and quality of life. It is worth emphasizing that excellent adherence of the applicator to the skin was observed resulting in the elimination of air gaps. This translates into precise delivery of the dose to the planned area.

In Figures 2 and 3, the appearance of the applicator in TPS and the printed applicator are presented. Catheters were attached to the applicator using heat-melt adhesive. Moreover, for each patient, to avoid the formation of air gaps and ensure consistency in the placement of the ap-

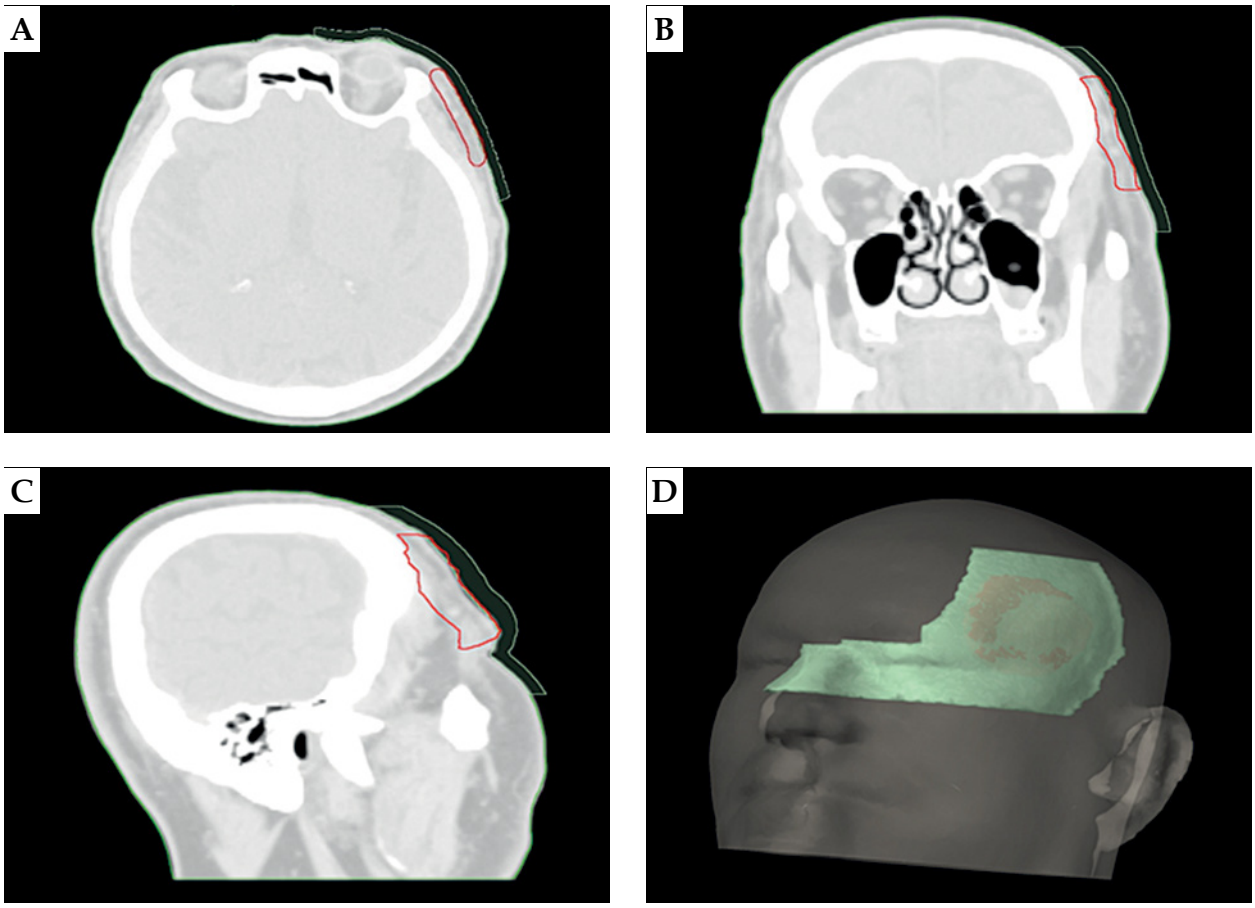

Fig. 2. View of CT scan with applicator and target structure for **A**) transverse section, **B**) frontal section, and **C**) sagittal section. **D**) 3D view

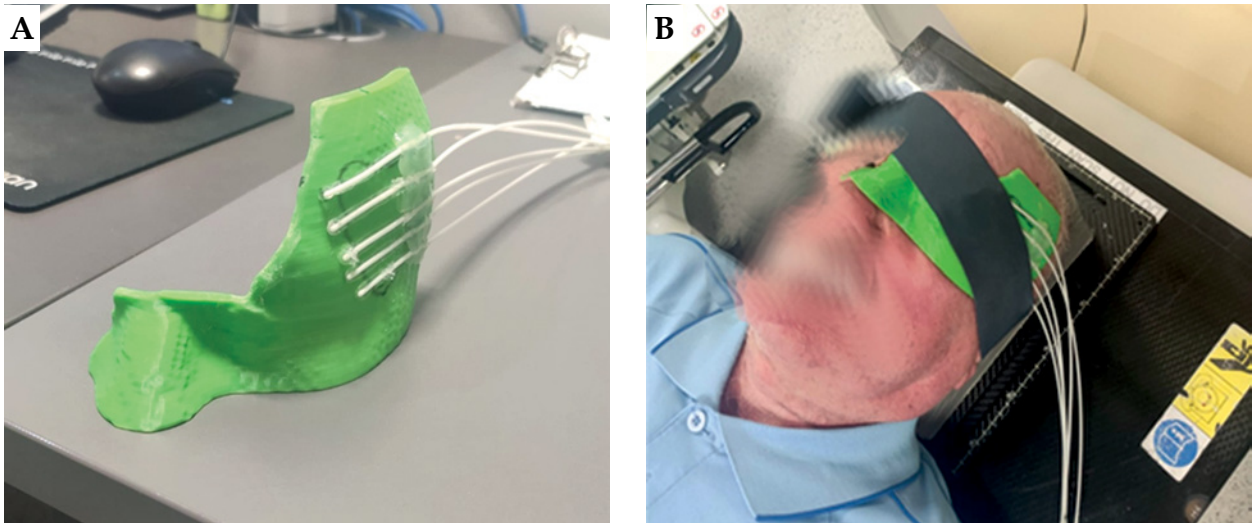

Fig. 3. A) 3D-printed applicator with catheters fixed with heat-melt adhesive. **B**) Picture of the patient with applicator fixed within the part of cancer-affected skin

Table 1. Comparison of treatment plan parameters with data of materials used

	Applicator displacement (cm)	V_{100} (%)	V_{150} (%)	D_{90} (Gy)	V_{PTV} (cm^3)	CI (–)	Total treatment time for 10 Ci (s)	Number of catheters (–)	Material used for applicator (g)	Filament length used for applicator (m)	3D printing time (h:m)
Patient 1	0.35 ±0.64	96.17	54.09	56.87	1.36	0.96	56	4	35	4.48	5:06
Patient 2	0.03 ±0.05	98.67	35.17	56.35	15.39	0.97	169	5	56	7.08	6:27
Patient 3	0.06 ±0.05	98.03	42.89	56.25	0.54	0.78	46	2	40	5.02	4:21
Patient 4	0.08 ±0.07	99.47	56.77	59.50	4.63	0.97	75	3	77	9.42	6:40
Patient 5	0.15 ±0.09	92.57	39.20	52.31	0.14	0.64	26	1	54	6.82	5:56

plicator during subsequent therapeutic fractions, a compression strip was applied. This prevented applicator movement during therapy session.

Treatment plan parameters and 3D-printed materials

During the treatment plan adjustment, a number of parameters was collected and summarized in Table 1.

For each patient, data on the repeatability of applicator position (displacement), treatment plan parameters (V_{100} (%), V_{150} (%), D_{90} (Gy), V_{PTV} (cm^3), CI, treatment time), and parameters related to the manufactured applicator (number of catheters, mass and length of the material used to produce the applicator, and printing time) were considered. By analyzing the data from Table 1, it can be concluded that the repeatability of the applicator positioning was very high, which has been proven in our previous work, where the results of 20 treatment plans were analyzed [34]. It should be noted that the size of cancer lesion (calculated as V_{PTV}) did not significantly affect the number of catheters used, and there was no significant correlation between the size of cancer lesion and the amount of material used to produce the applicator as well as printing time. The size of the applicator was mainly influenced by the geometry of the cancerous part of the body. It is important that a small amount of material was used to prepare the applicator (< 100 g), and the printing time did not exceed 7 hours. This was a fully automated process, eliminating the need for the presence of personnel.

Results of clinical observations of patients during and post-radiotherapy

Evaluation with RTOG scale

The Radiation Therapy Oncology Group scale (RTOG scale) is an instrument to evaluate the severity of side effects or complications experienced by patients undergoing radiation therapy for cancer treatment. This scale provides standardized criteria for assessing and grading the severity of adverse events, such as skin reactions. The RTOG scale helps clinicians communicate effectively about treatment-related toxicities as well as facilitates comparisons of different clinical trials and treatment protocols. In Table 2, the RTOG scoring criteria are presented [35].

Patient No. 1

First appointment: On the earlobe of the right auricle, there was a visible superficial flat ulceration measuring 2.0 × 1.5 cm, extending onto the skin of the neck behind the ear. Lymph nodes were intact.

First follow-up: On the earlobe of the right auricle, there was moist desquamation in the irradiated area. RTOG scale – grade 3.

Second follow-up: A visible dry scab present on the earlobe of the left auricle in the radiated area. Healing status was graded as 2 according to RTOG.

Third follow-up: The skin of the right auricle was completely healed, with no pain on palpation. Complete remission was observed, with no post-radiation reaction. RTOG scale – grade 0.

In Figure 4, images captured during the patient four consecutive visits are presented.

Patient No. 2

First appointment: On the left temple, there was an irregular patch of depigmented skin with pinpoint redness. Adjacent to the outer end of the left eyebrow, there was a slightly raised nodule with a superficial ulceration measuring 1.0 × 1.0 cm. Loco-regional lymph nodes were intact.

First follow-up: On the left temple within the irradiated skin area, there was a reaction characterized by moist desquamation of the epidermis and a localized ulceration measuring 2.0 × 2.0 cm, graded as 3 as per RTOG scale. According to the patient, the area of reaction was decreasing in size over several days.

Table 2. RTOG scoring criteria for skin changes [35]

RTOG scoring criteria	Skin changes
0	No change over baseline
1	Follicular, faint or dull erythema, epilation, dry desquamation, decreased sweating
2	Tender or bright erythema, patchy moist desquamation, moderate oedema
3	Confluent, moist desquamation other than skin folds, pitting oedema
4	Ulceration hemorrhage, necrosis

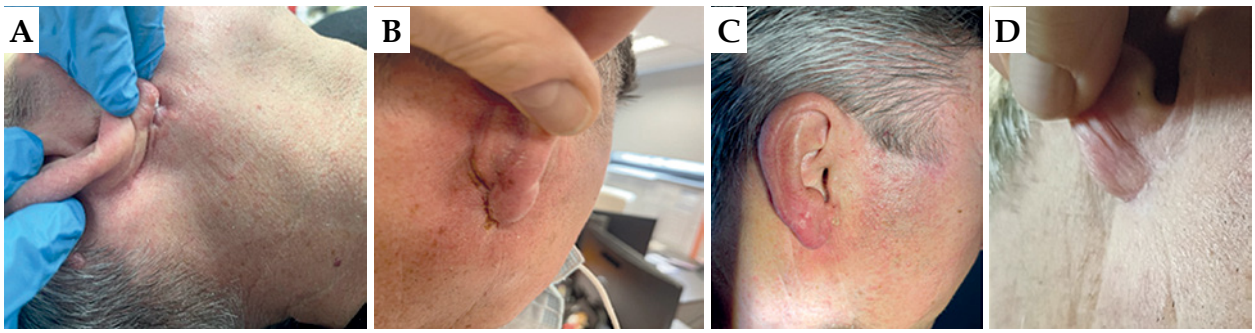

Fig. 4. Patient No. 1 treatment progress. **A**) First appointment; **B**) First follow-up (2 months); **C**) Second follow-up (3 months); **D**) Third follow-up (6 months)

Second follow-up: On the left temple, the skin in the irradiated area was 90% healed, with a remaining wound centrally within the irradiation field measuring 1.5 × 1.5 cm in the form of a skin-level ulceration. RTOG scale – grade 3.

Third follow-up: Complete remission was observed on the left temple, with the skin in the irradiated area fully healed and the tumor absent. Palpation revealed softness and non-suspicious findings. RTOG scale – grade 0.

Figure 5 shows pictures of the left temple during each of the described above visits.

Patient No. 3

First appointment: The ulcerating lesion was located approximately 2.0 cm from the outer corner of the left eye on the cheek, measuring 2.0 × 1.0 cm, with an endophytic character. Loco-regional lymph nodes were intact.

First follow-up: The ulcerating lesion remained located approximately 2.0 cm from the outer corner of the left eye on the cheek, measuring 2.0 × 1.0 cm, with an endophytic character. RTOG scale – grade 4.

Second follow-up: Complete remission of the disease was observed. In the treated area, the skin was fully healed, slightly reddened, soft to the touch, without any thickening. RTOG scale – grade 0.

Third follow-up: Complete remission of the disease was maintained. In the treated area, the skin was fully healed, palpably very smooth, and slightly depigmented. RTOG scale – grade 0.

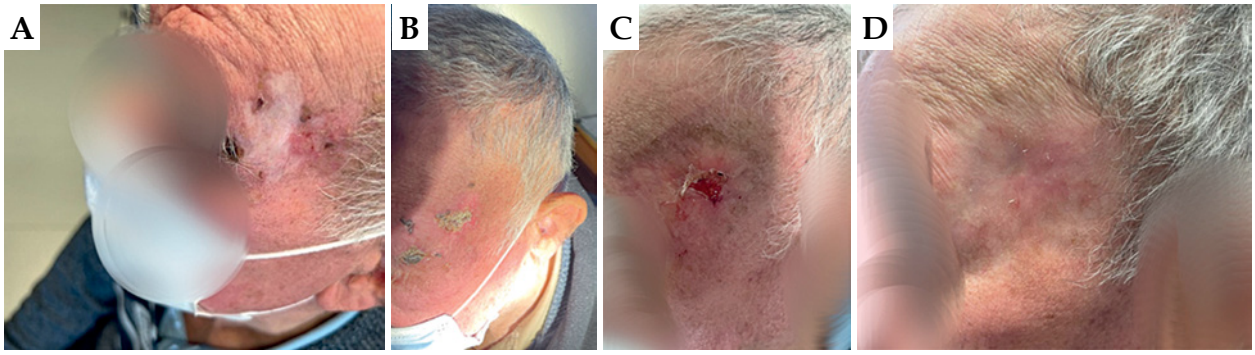

Fig. 5. Patient No. 2 treatment progress. **A**) First appointment; **B**) First follow-up (2 months); **C**) Second follow-up (3 months); **D**) Third follow-up (6 months)

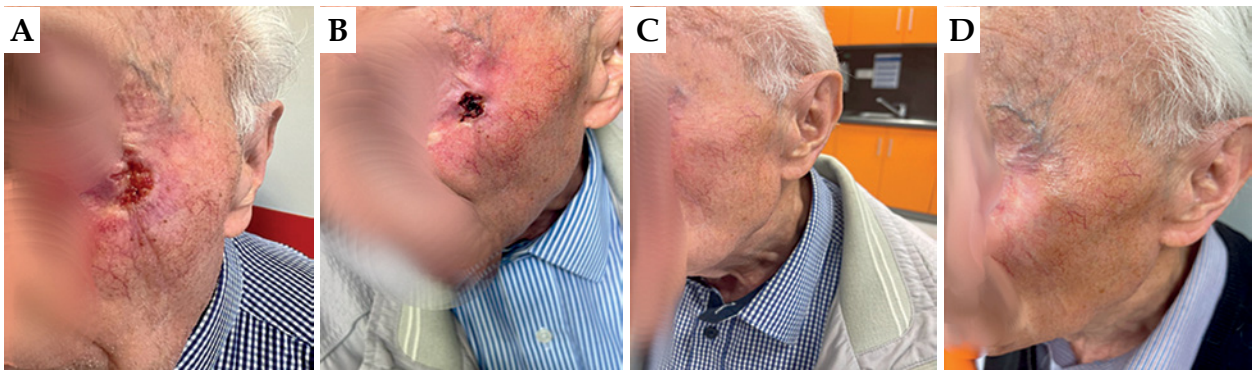

Fig. 6. Patient No. 3 treatment progress. **A**) First appointment; **B**) First follow-up (2 months); **C**) Second follow-up (3 months); **D**) Third follow-up (6 months)

In Figure 6, patient pictures taken during the 4 visits are presented.

Patient No. 4

First appointment: On the internal surface of the right hand, a visible and palpable irregular, slightly raised tumor with a superficial, yellowish ulceration measuring 3.0 × 3.0 cm was observed. Loco-regional lymph nodes were intact.

First follow-up: On the internal surface of the right hand, an oval ulceration measuring 3.0 × 3.0 cm was visible, with moist desquamation of the epidermis. According to the patient, the ulceration was itchy. RTOG scale – grade 3.

Second follow-up: On the internal surface of the right hand, an oval dry ulceration measuring 2.5 × 2.5 cm was visible. RTOG scale – grade 2.

Third follow-up: On the internal surface of the right hand, no ulceration was present, and the skin at the treated site was very smooth. According to the patient, sensation was normal. RTOG scale – grade 0.

In Figure 7, images captured during the 4 patient visits are presented.

Patient No. 5

First appointment: On the right cheek, approximately 2.0 cm below the lower eyelid, an ulcerating nodule measuring approximately 0.5 × 0.5 cm was observed. It was slightly raised above the surface of the healthy skin. Loco-regional lymph nodes were intact.

First follow-up: On the right cheek, below the outer corner of the right eye, there was pinpoint discoloration of the skin with dry desquamation of the epidermis. RTOG scale – grade 1.

Second follow-up: On the right cheek, the site after treatment was difficult to locate without the access to patient documentation. There was a small spot at the site of the primary lesion. Very good cosmetic effect, with not suspicious skin palpation and inspection. RTOG scale – grade 0.

Third follow-up: On the right cheek, the skin in the irradiated area was unchanged in color, with a small discolored spot at the site of the primary lesion. RTOG scale – grade 0.

In Figure 8, images of the patient during the four visits are presented.

Dermatoscopy and video-dermatoscopy

Considering the clinical picture during radiotherapy, there can be an inflammatory reaction around the tumor and surrounding skin that shows positioning of the overlay vs. cancerous change. Usually, it is central ulcer with serous secretion. Four weeks after completing treatment, the changes regressed: the sore healed and the size of the tumor reduced. Three months after the treatment, clin-

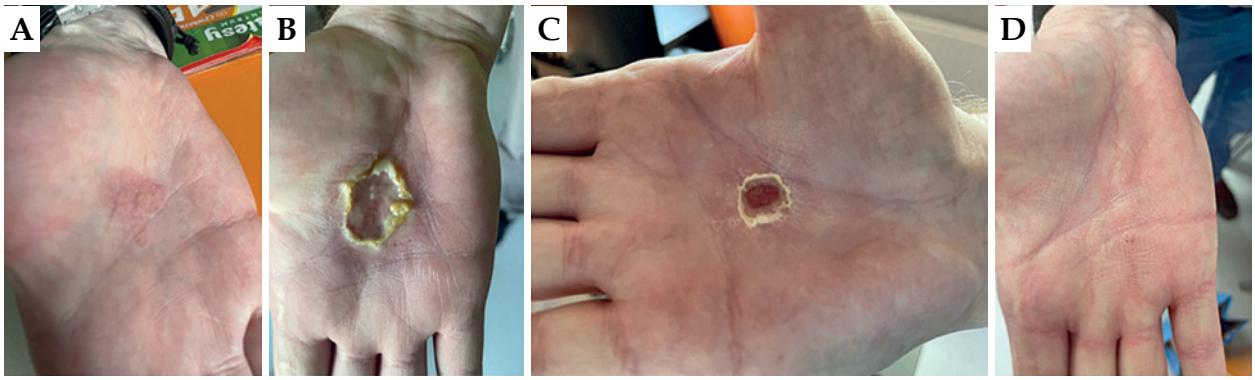

Fig. 7. Patient No. 4 treatment progress. **A**) First appointment; **B**) First follow-up (2 months); **C**) Second follow-up (3 months); **D**) Third follow-up (6 months)

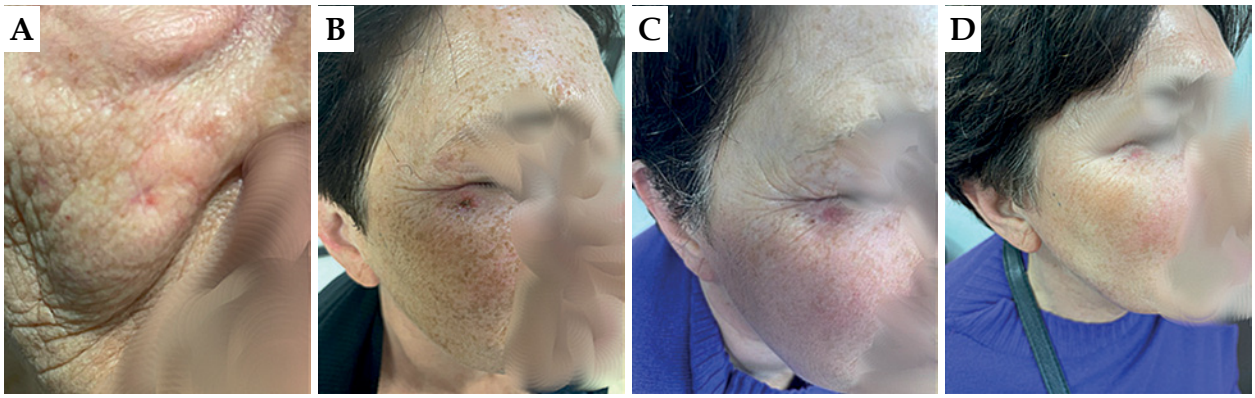

Fig. 8. Patient No. 5 treatment progress. **A**) First appointment; **B**) First follow-up (2 months); **C**) Second follow-up (3 months); **D**) Third follow-up (6 months)

ically, no exophytic was observed, neither any tumor, scabs, or endophytic changes, such as ulcers. Any residue that might be noticed was a post-inflammatory erythema that appeared in the post-tumor area. When dermatoscopy and video-dermatoscopy were viewed during radiotherapy, there was a big yellow papule that corresponded to dried serous secretion within the sore area. At four weeks after the irradiation, the above described papule was not observed. The intensity of inflammatory reaction was also reduced. Subsequently dermatoscopical structures disappeared: typical for basal cell carcinoma, i.e., ovoid nests, big blue papule, and arborising linear vessels (branch-like vessels), and typical for squamous cell carcinoma, i.e., polymorphic vessels, white wheels pink, amorphous structureless area. At 3 months after the treatment, in dermatoscopy and video-dermatoscopy, no typical BCC or SCC structures were observed. There might be visible only short and linear blood vessels on the pink background, which corresponded to the post-inflammatory erythema. Pictures were obtained with Medicum 800 (Vexia, FotoFinder, Germany).

Reflectance confocal microscopy (RCM)

Reflectance confocal microscopy was performed on the day of skin cancer diagnosis, before skin biopsy, and then 4 weeks and 12 weeks after brachytherapy treatment. On the initial RCM pictures, the typical neoplastic features were present. For basal cell carcinoma, dark silhouettes and bright tumor islands with surrounding dark clefting were observed. Dendritic cells were also visible within tumor islands as well as canalicular dilated vessels. For squamous cell carcinoma, atypical honeycomb pattern with parakeratosis and dyskeratosis features, cellular pleomorphism in spinous-granular layer, and numerous dilated blood vessels in coiled (glomerular) pattern were noted. In RCM examination performed four weeks after brachytherapy, exocytosis and/or spongiosis was observed. The presence of numerous dendritic cells within spinous-granular layer confirmed the inflammatory process in the skin induced by the radiation, in line with a previous study [36]. After 12 weeks of brachytherapy ending, RCM revealed normotypic epidermis without any sings of residual disease. In the dermis, a network of well-defined collagen bundles was observed, corresponding to a scar after radiotherapy in the site of previous tumor. In conclusion, reflectance confocal microscopy is a highly sensitive imaging tool for monitoring skin changes after brachytherapy of skin cancers. It enables avoiding unnecessary biopsies and controls residual disease in non-invasive manner.

Patient No. 5 is an example of using RCM in BCC therapy, and the following are the obtained results. Figure 9A and 9B demonstrate the area of stratum spinosum of the epidermis before and 12 weeks after the treatment. In Figure 9A, characteristic elongated keratinocytes typical for BCC can be observed, aligning along a single line seemingly embracing the underlying tumor, while in Figure 9B, a normal stratum spinosum is visible after healing post-HDR therapy. Figure 9C and 9D show the upper layers of the dermis in BCC before and 12 weeks after the irradiation. In Figure 9C, typical nests of basaloid cells interspersed with connective tissue septa, a characteristic for BCC, are visible. Figure 9D shows numerous collagen fibers indicating scarring process (a scar after completing HDR-BT treatment). RCM pictures were obtained using VivaScope® 1500 and 3000 (MAVIG GmbH, Munich, Germany).

Optical profilometry

During the fabrication of 3D-printed applicators, few aspects were taken into account which affected the final printout. Even though Ricotti *et al*. suggested that printout with lower infill percentage can be applied for high-dose-rate brachytherapy [33], all applicators were created with 100% infill, which on average increased the printing time by around 25% (as compared with 15% infill). For the applicator shown in Figure 10, the printing time for 15% infill with selected supports was 1 h 30 min, and increased to 1 h 59 min when 100% infill was set. Whenever the applicator .stl file was treated in slicer, the compromise between its printability with the least amount of the supports were considered. In this way, we wanted to avoid any potential sharp defects at the applicator surface, which could cause patient inconvenience. Figure 10A demonstrates the example of applicator .stl file (for the nasal area) uploaded to the dedicated slicer. Figure 10B represents the same image with dark blue regions being the applicators parts, which required the use of support. These parts were selected manually as the automatic generation of supports lead to excessive amount

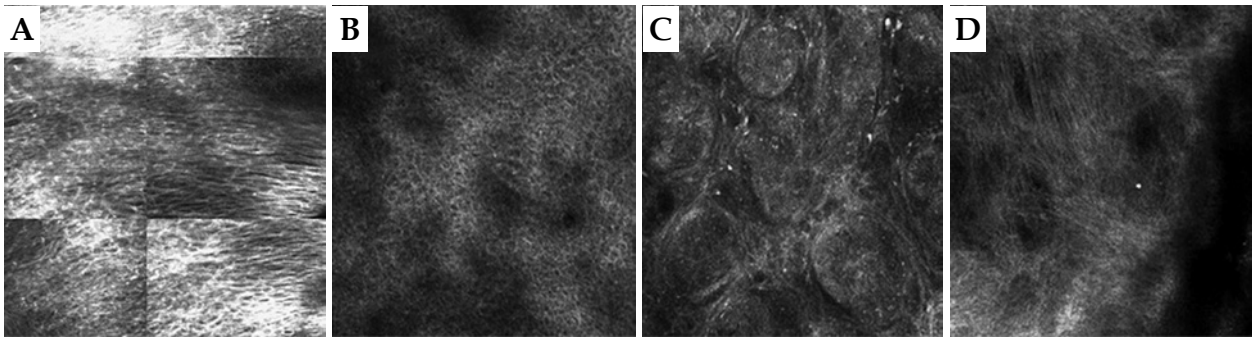

Fig. 9. Set of images using reflectance confocal microscopy. **A**) Epidermis before radiotherapy for BCC; **B**) Epidermis after 12 weeks of radiotherapy; **C**) Skin with BCC before radiotherapy; **D**) Scarred skin at 12 weeks after HDR-BT

of printed material contacting inner surface of the applicator. Custom selection of the applicator surface that require support reduce printing time, the amount of the used material, and most of all, diminish the surface area of the applicator that is prone to mechanical defects at the junction between support and applicator (Fig. 10C). Also, the micro-structures existing at the surface of the exemplary applicator were analyzed, as shown in Figure 10D. Since the thermoplastic is printed in layers, the extruded material leaves a micro-pattern on both sides of the printout (one facing the skin and the other with the source attached). It was found that these features have very repetitive manner, as the grove and hills are separated by around 100 micrometers (Fig. 10E-G). Nevertheless, the printout roughness along with the surface micro-pattern did not affect high-dose-rate brachytherapy delivery of radiation dose to cancer cells. The surface characteristics of the applicator may influence various factors, such as patient comfort and applicator stability.

Conclusions

In the current study, a comprehensive investigation of the efficacy of 3D-printed applicators for the treatment of inoperable skin cancer lesions was conducted. Five patients, with tumor lesions ineligible for surgical interventions located in various anatomical sites, were enrolled. Customized applicators were fabricated using 3D printing for each patient, ensuring precise conformity to individual anatomical features. Subsequently, patients underwent a radiotherapy protocol delivering a total dose of 51 Gy in 17 fractions. During and post-radiotherapy, patients were closely monitored using clinical assessments and advanced imaging techniques, such as dermatoscopy, video-dermatoscopy, and RCM. Treatment outcomes were assessed based on the RTOG scale, with complete remission observed uniformly in all the five patients. The clinical observation of each patient included the following timeline: first appointment, observation in all treatment fractions, first follow-up (2 months), second follow-up (3 months), and third follow-up (6 months). The study carefully evaluated treatment plan parameters, especially those significant for 3D printing, including V_{100} (%), V_{150} (%), D_{90} (Gy), V_{PTV} (cm^3), and CI parameter. Additionally, factors related to the manufacturing process of the applicators were analyzed, such as printing time, filament usage, and the number of catheters applied. Our findings demonstrate the potential of 3D-printed applicators to enhance therapeutic precision and patient outcome in skin cancer management. The integration of advanced imaging techniques provided valuable insights into treatment effects, including the regression of inflammatory reactions and the absence of residual disease. Notably, the study highlights the reproducibility of the applicator position, the minimal impact of cancer lesion size on the manufacturing parameters, and the importance of meticulous fabrication to ensure the applicator stability and patient comfort. Our study demonstrates the precise fabrication and evaluation of 3D-printed applicators for high-dose-rate brachytherapy in skin cancer treatment.

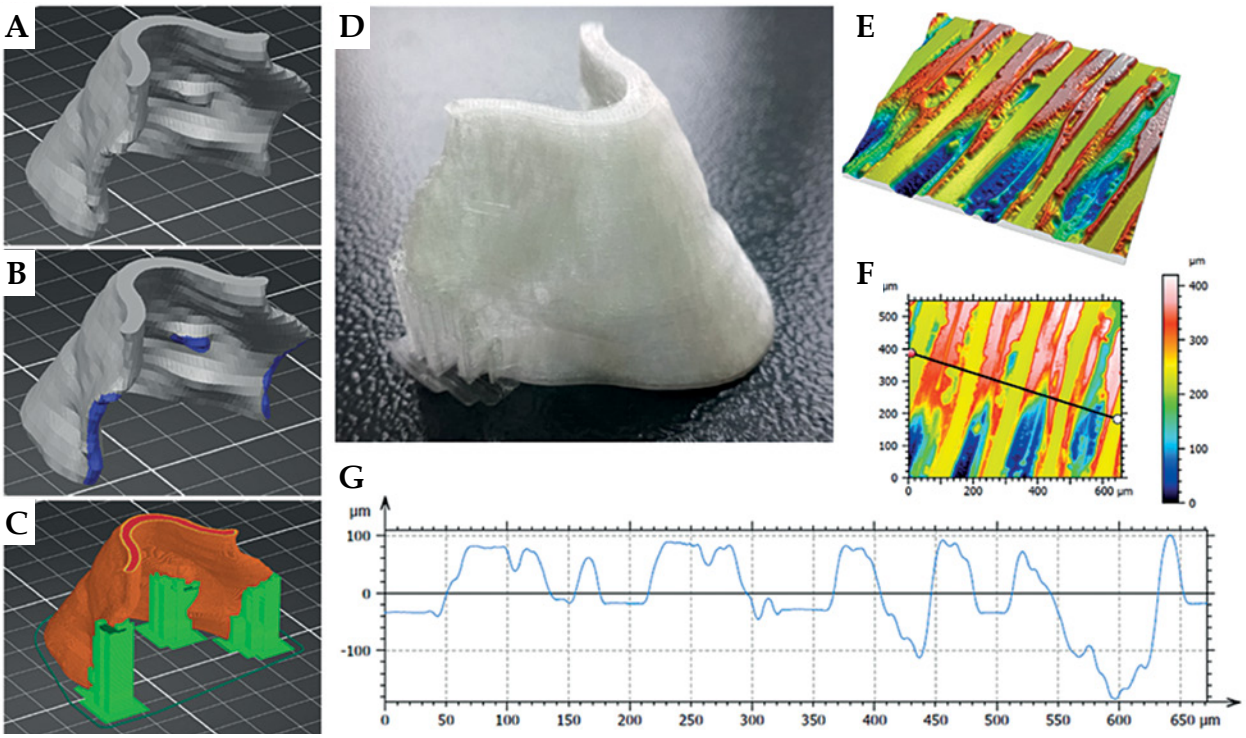

Fig. 10. A) .stl file of the applicator opened in Prusa Slicer software; **B**) Applicator with regions (indicated with blue color), which require printing supports; **C**) Sliced applicator (orange) with supports (green); **D**) Picture of 3D-printed applicator; **E**, **F**) The images recorded with the optical profilometry microscopy as 3D and 2D maps, respectively (scale bar is shown in the right panel of E); **G**) The line profile of the applicator that corresponds to the section marked with the black line in (**E**)

Despite opting for 100% infill to ensure structural integrity, we minimized material usage and surface defects, enhancing patient comfort and applicator stability. Our findings support the feasibility and effectiveness of 3D-printed applicators in improving treatment outcomes for skin cancer patients undergoing brachytherapy.

In conclusion, the personalized approach facilitated by 3D-printed applicators offers a promising avenue for improving the quality of care for patients with inoperable skin cancer lesions. By optimizing treatment planning parameters and enhancing therapeutic precision, this approach has the potential to minimize treatment-related side effects and improve overall patient outcome. Further research and clinical validation are warranted to validate these findings, and establish 3D printing as a standard practice in skin cancer treatment. Close collaboration between radiotherapists, medical physicists, and dermatologists experienced in skin imaging techniques can result in therapeutic success of skin cancer brachytherapy.

Funding

This research received no external funding.

Disclosures

The study was approved by Bioethics Committee of the Centre of Postgraduate Medical Education (approval No. 119/2023 issued on April 5, 2023).

The authors report no conflict of interest.

References

1. Guinot JL, Rembielak A, Perez-Calatayud J et al. GEC-ESTRO ACROP recommendations in skin brachytherapy. *Radiother Oncol* 2018; 126: 377-385.
2. Skowronek J. Brachytherapy in the treatment of skin cancer: An overview. *Postepy Dermatol Alergol* 2015; 32: 362-367.
3. Rowe DE, Carroll RJ, Day CL. Mohs surgery is the treatment of choice for recurrent (previously treated) basal cell carcinoma. *J Dermatol Surg Oncol* 1989; 15: 424-431.
4. Rowe DE, Carroll RJ, Day CL. Prognostic factors for local recurrence, metastasis, and survival rates in squamous cell carcinoma of the skin, ear, and lip. Implications for treatment modality selection. *J Am Acad Dermatol* 1992; 26: 976-990.
5. Guix B, Finestres F, Tello JI et al. Treatment of skin carcinomas of the face by high-dose-rate brachytherapy and custom-made surface molds. *Int J Radiat Oncol Biol Phys* 2000; 47: 95-102.
6. Kowalik Ł, Łyczek J, Sawicki M et al. Individual applicator for brachytherapy for various sites of superficial malignant lesions. *J Contemp Brachytherapy* 2013; 5: 45-49.
7. Gauden R, Pracy M, Avery AM et al. HDR brachytherapy for superficial non-melanoma skin cancers. *J Med Imaging Radiat Oncol* 2013; 57: 212-217.
8. Ghaly M, Dannenberg H, Satchwill K et al. HDR brachytherapy with standardized surface applicators in the treatment of superficial malignant skin lesions. Volume 72, Issue 1, Supplement, S505-S506, September 01, 2008.
9. Niu H, His WC, Chu JCH et al. Dosimetric characteristics of the Leipzig surface applicators used in the high dose rate brachy radiotherapy. *Med Phys* 2004; 31: 3372-3377.
10. Köhler-Brock A, Prager W, Pohlmann S et al. The indications for and results of HDR afterloading therapy in diseases of the skin and mucosa with standardized surface applicators (the Leipzig applicator). *Strahlenther Onkol* 1999; 175: 170-174.
11. Bray F, Ferlay J, Soerjomataram I et al. Global cancer statistics 2018: GLOBOCAN estimates of incidence and mortality worldwide for 36 cancers in 185 countries. *CA Cancer J Clin* 2018; 68: 394-424.
12. Bath-Hextall F, Leonardi-Bee J, Smith C et al. Trends in incidence of skin basal cell carcinoma. Additional evidence from a UK primary care database study. *Int J Cancer* 2007; 121: 2105-2108.
13. Madan V, Lear JT, Szeimies RM. Non-melanoma skin cancer. *Lancet* 2010; 375: 673-658.
14. Neville JA, Welch E, Leffell DJ. Management of nonmelanoma skin cancer in 2007. *Nat Clin Pract Oncol* 2007; 4: 462-469.
15. Rodriguez S, Santos M, Richart J et al. High-dose-rate brachytherapy in skin cancers: Patient convenience, local control and cosmetical results. *Brachytherapy* 2008; 7: 159.
16. Łogodziec W, Ślosarek K, Malicki J. Dose-rate distribution under partially shielded beams. *Strahlenther Onkol* 1990; 166: 733-737.
17. Poltorak M, Banatkiewicz P, Poltorak L et al. Brachytherapy and 3D printing for skin cancer: A review paper. *J Contemp Brachytherapy* 2024; 16: 156-169.
18. Gross B, Lockwood SY, Spence DM. Recent advances in analytical chemistry by 3D printing. *Anal Chem* 2017; 89: 57-70.
19. Capel AJ, Rimington RP, Lewis MP, Christie SDR. 3D printing for chemical, pharmaceutical and biological applications. *Nat Rev Chem* 2018. doi: 10.1038/s41570-018-0058-y.
20. Chia HN, Wu BM. Recent advances in 3D printing of biomaterials. *J Biol Eng* 2015; 9: 4.
21. Gauvin R, Chen YC, Lee JW et al. Microfabrication of complex porous tissue engineering scaffolds using 3D projection stereolithography. *Biomaterials* 2012; 33: 3824-3834.
22. Goh GL, Zhang H, Chong TH et al. 3D printing of multilayered and multimaterial electronics: A review. *Adv Electron Mater* 2021; 7.
23. Ali MH, Issayev G, Shehab E et al. A critical review of 3D printing and digital manufacturing in construction engineering. *Rapid Prototyp J* 2022; 28: 1312-1324.
24. Xu N, Ye X, Wei D et al. 3D artificial bones for bone repair prepared by computed tomography-guided fused deposition modeling for bone repair. *ACS Appl Mater Interfaces* 2014; 6: 14952-14963.
25. Lakkala P, Munnangi SR, Bandari S et al. Additive manufacturing technologies with emphasis on stereolithography 3D printing in pharmaceutical and medical applications: A review. *Int J Pharm X* 2023; 5: 100159.
26. Aljohani W, Ullah MW, Zhang X et al. Bioprinting and its applications in tissue engineering and regenerative medicine. *Int J Biol Macromol* 2018; 107: 261-275.
27. Eichholz KF, Pitacco P, Burdis R et al. Integrating melt electrowriting and fused deposition modeling to fabricate hybrid scaffolds supportive of accelerated bone regeneration. *Adv Healthc Mater* 2024; 13: e2302057.
28. Picco CJ, Utomo E, McClean A et al. Development of 3D-printed subcutaneous implants using concentrated polymer/drug solutions. *Int J Pharm* 2023; 631: 122477.
29. Kempin W, Franz C, Koster LC et al. Assessment of different polymers and drug loads for fused deposition modeling of drug loaded implants. *Eur J Pharm Biopharm* 2017; 115: 84-93.
30. Popov VV, Muller-Kamskii G, Kovalevsky G et al. Design and 3D-printing of titanium bone implants: brief review of approach and clinical cases. *Biomed Eng Lett* 2018; 8: 337-344.
31. Dekker TJ, Steele JR, Federer AE et al. Use of patient-specific 3D-printed titanium implants for complex foot and ankle limb salvage, deformity correction, and arthrodesis procedures. *Foot Ankle Int* 2018; 39: 916-921.

32. Huo W, Ding Y, Sheng C et al. Application of 3D printing in cervical cancer brachytherapy. *J Radiat Res Appl Sci* 2022; 15: 18-24.
33. Ricotti R, Vavassori A, Bazani A et al. 3D-printed applicators for high dose rate brachytherapy: Dosimetric assessment at different infill percentage. *Phys Med* 2016; 32: 1698-1706.
34. Poltorak M, Banatkiewicz P, Poltorak L et al. Quantitative dosimetric analysis with independent software solutions and comprehensive treatment plan parameter evaluation. *SSRN* 2024.
35. Wong S, Kaur A, Back M et al. An ultrasonographic evaluation of skin thickness in breast cancer patients after postmastectomy radiation therapy. *Radiat Oncol* 2011; 6: 9.
36. Kišonas J, Venius J, Grybauskas M et al. Acute radiation dermatitis evaluation with reflectance confocal microscopy: A prospective study. *Diagnostics* 2021; 11: 1670.